NeuroImage 336 (2026) 122007

Contents lists available at ScienceDirect

NeuroImage

journal homepage: www.elsevier.com/locate/ynimg

EEG microstates reveal differential network dynamics under constant current and oscillatory brain stimulation

Inga Griškova-Bulanova [a,*], Povilas Tarailis [a], Marko Živanović [b], Saša Filipović [c], Jovana Bjekić [c,*]

[a] Faculty of Medicine, Vilnius University, Translational Health Research Institute, Žalių ež. str. 2, Vilnius LT-08406, Lithuania
[b] Department of Psychology, Faculty of Philosophy, Institute of Psychology, University of Belgrade, Čika Ljubina 18-20, Belgrade, Serbia
[c] Centre for Neuroscience and Neuromodulation, University of Belgrade, Institute for Medical Research, Dr Subotića 4, POB 39, Belgrade, Serbia

ARTICLE INFO

Keywords:
EEG microstates
Transcranial electrical stimulation (tES)
Transcranial direct current stimulation (tDCS)
Transcranial alternating current stimulation (tACS)
Oscillatory tDCS (otDCS)
Individualized theta frequency
Neuromodulation
Resting-state EEG

ABSTRACT

Background: EEG microstates are brief, quasi-stable scalp topographies that index large-scale network dynamics and may sensitively capture the net effects of transcranial electrical stimulation (tES).
Objective: To evaluate differential effects of three types of tES - tDCS, tACS and oscillatory tDCS (otDCS) on canonical EEG microstates (A-D) in healthy adults.
Methods: In a randomized, sham-controlled, crossover study, 42 participants completed four sessions (tDCS, tACS, otDCS, sham). Stimulation (20 min) used a P3–cheek montage: tDCS +1.5 mA; tACS at individualized theta frequency (ITF, 4–8 Hz), ±1 mA; otDCS anodal with ±0.5 mA oscillation around +1.5 mA at ITF. A five-minute resting EEG (eyes closed then eyes open) was recorded pre- and post-intervention. Microstates were extracted (A–D), back-fitted, and assessed on duration, occurrence, contribution, and mean GFP using linear mixed-effects models with sham and pre/post adjustments.
Results: Four canonical microstates explained ~80% of the variance with stable topographies across conditions. Modulation patterns were modality-specific. MS A (sensory/arousal) increased across all active protocols, strongest after otDCS. MS B (visual-autobiographical) was consistently suppressed, again most following otDCS. MS C (self-referential) decreased selectively after oscillatory stimulation (tACS, otDCS) only. MS D (executive/attention) diverged by waveform: enhanced by tACS and otDCS but reduced by tDCS. Across outcomes, otDCS produced the largest and most widespread effects with overlapping features of both tDCS (tonic/stabilizing) and tACS (oscillatory/entraining).
Conclusions: Resting-state EEG microstates provide a sensitive systems-level assay of tES aftereffects. Constant and oscillatory current waveforms affect network states in dissociable ways, with otDCS exerting the most robust, comprehensive modulation. These findings support microstates as practical biomarkers for differentiating, optimizing, and monitoring neuromodulation strategies.

1. Introduction

Low-intensity transcranial electrical stimulation (tES) has become widely used for investigating and modulating human brain function in a non-invasive manner. By delivering weak currents through the scalp, tES protocols can interact with ongoing neuronal activity in distinct ways. Among the major tES modalities, transcranial direct current stimulation (tDCS) induces polarity-dependent shifts in cortical excitability via constant currents (Woods et al., 2016; Nitsche and Paulus, 2000; Filmer et al., 2014), while transcranial alternating current stimulation (tACS) applies rhythmic stimulation to entrain, shift, or interfere with endogenous oscillations (Antal and Paulus, 2013; Elyamany et al., 2021; Agboada et al., 2025). Oscillatory transcranial direct current stimulation (otDCS), is a relatively novel technique that combines these approaches by embedding a sinusoidal component within a steady DC offset, potentially integrating excitability shifts with oscillatory entrainment (Vulić et al., 2021; Guo et al., 2025; Wischnewski et al., 2026; Živanović et al., 2022).

Effective use of tES depends on the precise understanding of how externally applied currents reshape intrinsic patterns of brain activity. A

* Corresponding authors.
E-mail addresses: inga.griskova-bulanova@gf.vu.lt (I. Griškova-Bulanova), jovana.bjekic@imi.bg.ac.rs (J. Bjekić).

https://doi.org/10.1016/j.neuroimage.2026.122007
Received 16 October 2025; Received in revised form 4 May 2026; Accepted 15 May 2026
Available online 16 May 2026

central challenge lies in determining how different stimulation modalities affect large-scale brain dynamics, rather than only local excitability or frequency-specific activity. Resting-state EEG provides one way to capture such dynamics through microstates - brief, quasi-stable topographies of brain activity lasting tens to hundreds of milliseconds (Michel and Koenig, 2018). Microstates are typically classified into four canonical classes (A, B, C, and D), each characterized by a distinct scalp topography and functional association. Their temporal parameters, including duration, occurrence, and contribution, are increasingly recognized as indices of functional brain states linked to cognition and clinical conditions (Michel and Koenig, 2018), making them a particularly suitable system-level outcome for studying the network-level aftereffects of tES.

EEG microstates offer a particularly useful framework for tracking the effects of brain stimulation because they provide a temporally precise index of large-scale brain network dynamics (Michel and Koenig, 2018; Custo et al., 2017). Unlike traditional oscillatory analyses that focus primarily on local or frequency-specific activity, microstates capture transient, quasi-stable topographies that reflect the coordinated activity of distributed functional networks such as the salience, default mode, attention, and executive control systems (Britz et al., 2010; Tarailis et al., 2024). This network-level sensitivity makes microstates particularly suitable for neuromodulation studies, where interventions are expected to induce network-level reorganizations rather than isolated local changes (Croce et al., 2018; Zhang et al., 2025; Gao et al., 2025). Across both clinical and healthy populations, microstate parameters have been shown to differentiate between pathological and typical brain function (Vass et al., 2025) and to change following effective stimulation, closely paralleling improvements in pain, mood, cognition, or psychiatric symptoms (Nishida et al., 2025; Gold et al., 2022; Hanoglu et al., 2022). If proven sensitive to stimulation-induced reorganization and clinical outcome, microstates could serve as cost-effective, accessible biomarkers that bridge mechanistic understanding and therapeutic monitoring of brain stimulation effects.

Despite this potential and their growing application in clinical neuroscience, evidence on how microstates reflect the effects of brain stimulation remains scarce. Initial findings with tDCS suggest that microstates are sensitive to stimulation-induced changes: in healthy participants, tDCS over motor and prefrontal regions reorganized network states linked to pain and anxiety (Zhang et al., 2025), while in autism spectrum disorder and depression, stimulation over the DLPFC increased the presence of functionally relevant microstates and aligned with symptom improvement (Nishida et al., 2025; Kang et al., 2023). In obsessive-compulsive disorder, orbitofrontal tDCS normalized aberrant microstate transitions, with microstate C emerging as a potential biomarker of therapeutic response (Cheng et al., 2024). More recently, in schizophrenia, repeated HD-tDCS delivered during working memory training increased the presence of MS B, which was reduced at baseline relative to controls, indicating a normalization of disorder-specific network alterations (Qin et al., 2025). These early studies highlight microstates as a promising, yet still underexplored, approach to track the large-scale brain effects of tDCS, while also supporting their broader relevance as a systems-level readout of stimulation-induced network reorganization.

Even fewer studies have examined the effects of tACS on EEG microstates, but the initial findings indicate that this approach can reveal stimulation-induced network reorganization. In healthy adults, γ-tACS at 40 Hz over DLPFC was shown to reduce the presence of microstate C and increase microstates D and B, with these changes correlating with enhanced working memory performance (Gao et al., 2025). Similarly, another study reported a consistent decrease in microstate C and an increase in microstate D following γ-tACS, highlighting the sensitivity of microstate analysis to capture large-scale effects of rhythmic brain stimulation (Gao et al., 2022). Despite the limited literature, investigating tACS effects on EEG microstates is conceptually well justified, as tACS is expected to influence ongoing oscillatory activity and large-scale network organization (Wischnewski et al., 2023).

Together, these findings position EEG microstates as a promising yet underutilized tool for probing stimulation-induced changes in large-scale brain networks. To advance this line of research, we conducted the first within-subject, systematic comparison of three commonly used and closely related tES modalities (tDCS, tACS, and otDCS) against sham condition, examining their effects on canonical EEG microstates. These modalities were selected because they permit a conceptually informative comparison of constant-current (tDCS), polarity-reversing oscillatory (tACS), and offset-oscillatory stimulation (otDCS) within the same experimental framework. The study aims to identify modality-specific signatures of network reorganization, thereby providing novel insights into the network-level effects of different tES modalities, while also evaluating the sensitivity of EEG microstates as a marker for differentiating the large-scale effects of distinct stimulation protocols.

2. Methods

2.1. Design

This study employed a sham-controlled, randomized, crossover tES-EEG experimental design and was conducted as part of the larger MEMORYST project (for details, see Bjekić et al., 2022). Namely, each participant completed four experimental sessions, at least one week apart to avoid potential carryover effects. In a counterbalanced order, they received one of four tES conditions: tDCS, otDCS, tACS, or sham. All key stimulation parameters other than waveform (i.e., electrode type and positions, duration) were held constant across all conditions to isolate modality-specific effects. Stimulation was delivered concurrently with cognitive tasks designed to standardize the level and type of cognitive engagement across participants. Resting-state EEG was recorded for 5 min immediately before and after each stimulation modality, beginning with 3 min of eyes-closed, followed by 2 min of eyes-open recording. The study was conducted in accordance with the Declaration of Helsinki and approved by the Institutional Ethics Board (EO129/2020).

2.2. Participants

The study recruited healthy young adults of both sexes who met the inclusion criteria and agreed to participate in exchange for monetary compensation (€8/hour). Individuals who expressed interest were first screened using an online eligibility self-assessment checklist. Inclusion criteria required participants to be right-handed, aged between 20 and 35 years, with normal or corrected-to-normal vision. Exclusion criteria included a history of seizures, neurological or psychiatric disorders, cognitive or learning disabilities, traumatic brain injury, metal implants in the head, chronic or acute dermatological conditions on the head, confirmed or suspected pregnancy, and current use of psychoactive substances or medications. These criteria were selected to minimize major participant-level factors that could confound EEG recordings or alter responsiveness to tES.

A total of 42 participants (26 female), aged 22–34 years ($M = 25.05$, $SD = 3.55$), were enrolled in the study. An a priori power analysis was conducted using G*Power software (Faul et al., 2007) to determine the appropriate sample size. Assuming a within-subjects design with four conditions, $\alpha = 0.05$, and power $(1 - \beta) = 0.80$, a minimum of 36 participants was required to detect a medium effect size ($f = 0.25$). The final sample size of 42 reflects deliberate oversampling to ensure adequate power despite potential attrition and signal quality issues common in tES-EEG research.

2.3. Transcranial electrical stimulation and EEG acquisition

Starstim32 system (Neuroelectrics Inc., Barcelona, Spain), a lightweight, mobile, battery-powered device remotely operated via the

Neuroelectrics® Instrument Controller (NIC2) software, was used for both tES delivery and EEG recording. The electrodes were secured using a neoprene cap with a 39-channel grid based on a subset of the international 10–10 EEG system. The EEG-tES setup is presented in Fig. 1 (panel A), alongside the visualization of the induced e-fields (panel C).

For stimulation, round rubber electrodes (25 cm^2) were inserted into saline-soaked sponge pockets. One electrode was placed over the left posterior parietal cortex (P3), and the other electrode was fixed to the contralateral cheek using medical adhesive tape (Fig. 1, panel B). This montage was selected to keep stimulation site constant across protocols while targeting a left posterior parietal region strongly implicated in memory, attentional control, and large-scale integrative processing (Bjekić et al., 2022), and because its relatively widespread field distribution makes it suitable for probing network-level aftereffects using EEG microstates. Stimulation lasted 20 min across all conditions, as this commonly used single-session tES duration is generally considered sufficient to induce measurable aftereffects without transitioning into the negative portion of the dose-response curve (Nitsche and Paulus, 2000). Anodal tDCS was delivered as a constant +1.5 mA current. tACS was applied at the individual theta frequency (ITF, 4–8 Hz) as a ± 1 mA sinusoidal waveform (2 mA peak-to-peak). otDCS used an anodal waveform oscillating ±0.5 mA around +1.5 mA (i.e., +1 to +2 mA) at ITF. The ITF was selected a priori as a fixed frequency parameter across oscillatory conditions, based on its relevance for large-scale memory and executive-control networks, and was also used as a personalization strategy to mitigate the between-subject variability commonly observed in tES effects (Bjekić et al., 2022). All active protocols included 30-second ramp-up and ramp-down periods. In the sham condition, current was applied for 60 s at the beginning and the end, using a 30-second ramp-up to 1.5 mA followed by a 30-second ramp-down.

EEG was recorded using 19 Ag/AgCl gel electrodes (4 mm diameter, 1 cm^2 gel-contact area) positioned at Fp1, Fp2, Fz, F3, F4, F7, F8, T7, T8, Cz, C3, C4, CP5, CP6, Pz, P4, PO7, PO8, and Oz. This electrode configuration was chosen to provide broad cortical coverage while avoiding physical overlap with stimulation sites. Reference and ground were provided by either a dual CMS/DRL ear-clip electrode attached to the right earlobe or two pre-gelled sticktrodes placed on the right mastoid (CMS) and just below it (DRL). EEG signals were recorded at a sampling rate of 500 Hz, with a bandwidth of 0–125 Hz (DC-coupled), 24-bit resolution, and a voltage resolution of 0.05 μV.

Data was manually preprocessed in the MATLAB environment using EEGLAB functions (Delorme and Makeig, 2004). The signals were first band-pass filtered between 1 and 40 Hz using a zero-phase, non-causal finite impulse response (FIR) filter applied in a two-pass forward and reverse manner, followed by removal of 50 Hz power line noise. Artefacts related to eye blinks, eye movements, and cardiac activity were corrected using Infomax-based independent component analysis (ICA). Noisy electrodes were removed and subsequently interpolated using a 3D spherical spline method. Finally, the data were re-referenced to the common average across all channels.

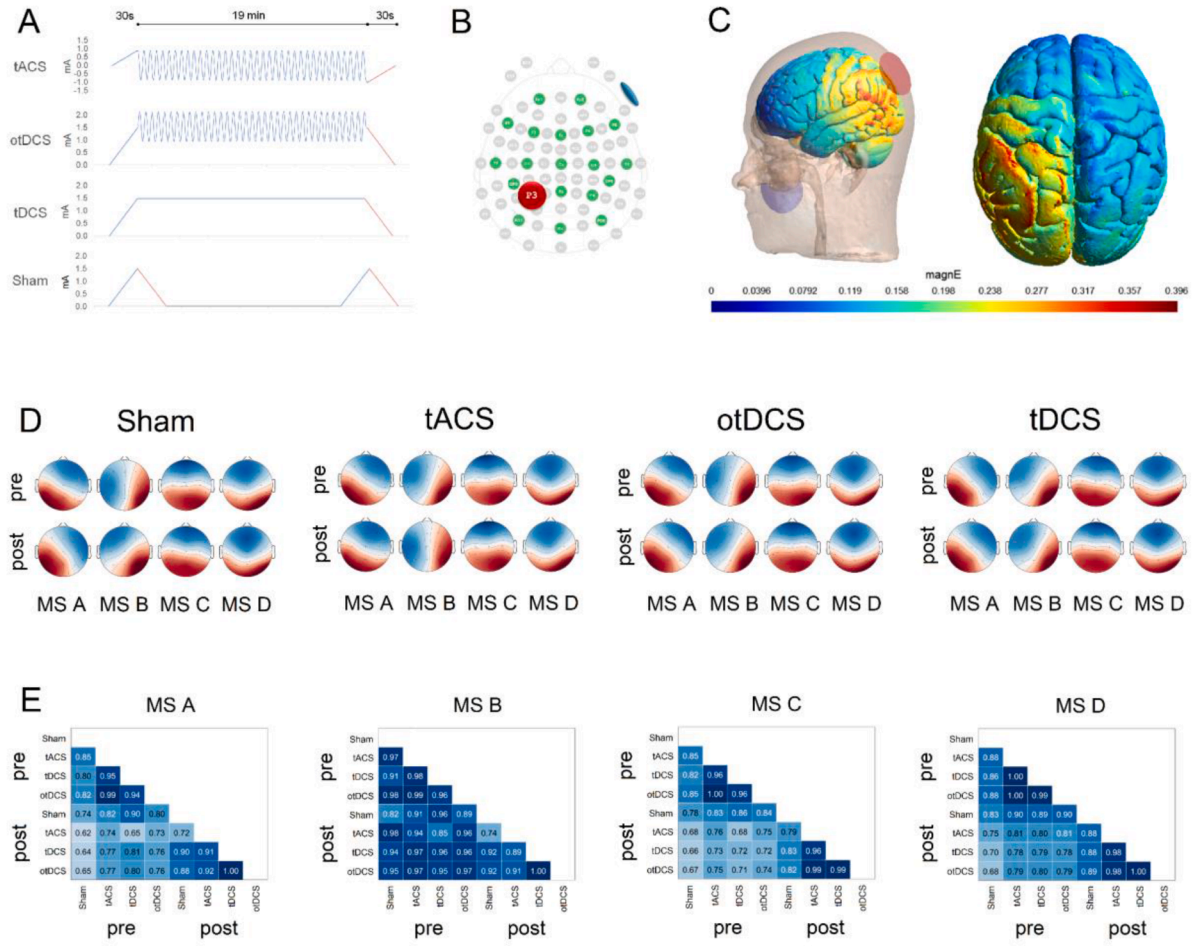

Fig. 1. (A) Overview of the stimulation protocols: tACS (30 s ramp-up to 1 mA, 19 min at ITF, 30 s ramp-down), otDCS (30 s ramp-up to 1.5 mA, 19 min at 1.5 ± 0.5 mA at ITF, 30 s ramp-down), tDCS (30 s ramp-up to 1.5 mA, 19 min at 1.5 mA, 30 s ramp-down), and sham (30 s ramp-up/down to 1.5 mA, 19 min at 0 mA, followed by a second 30 s ramp-up/down). (B) tES–EEG electrode setup. (C) SimNIBS simulation of the induced electric field for 1.5 mA current intensity. (D) Group-level topographies of the four canonical microstates extracted pre- and post-stimulation for each condition (sham, tDCS, tACS, and otDCS). (E) Spatial correlation coefficients for each microstate class between group-level topographies across stimulation conditions.

2.4. EEG analysis

Only eyes-closed data was used in this report. The EEG analysis focused on canonical resting-state microstates as a systems-level measure of stimulation-induced changes in large-scale brain dynamics. The microstate analysis was performed using a microstate plugin for EEGLAB (Nagabhushan Kalburgi et al., 2024) and custom-written functions. Since the present study used resting-state EEG microstate analysis, the relevant analytical steps concerned the extraction of Global Field Power (GFP), clustering of scalp topographies, backfitting, and quantification of standard microstate parameters.

For each condition (Sham, tDCS, tACS, otDCS), data were analyzed in two steps: at the individual and at the group levels. First, for each subject, GFP was calculated. To ensure a sufficient signal-to-noise ratio, only the maps at momentary peaks of the GFP were extracted (Koenig and Brandeis, 2016; Zanesco, 2020) and submitted to a modified k-means clustering algorithm (Pascual-Marqui et al., 1995), ignoring polarity differences. For each subject, the number of clusters ranged between 2 and 8, and to maximize global explained variance (GEV), clustering was repeated 50 times for each number of clusters. For the second step, individual topographies at each number of clusters were averaged across participant group-wise, using a permutation algorithm that maximizes the common variance between subjects (Koenig et al., 1999). The optimal number of group-level topographies for each condition was estimated as 4 based on the Silhouette method (Rousseeuw, 1987; Tarailis et al., 2021). To quantify the spatial similarity between the groups, spatial correlation was calculated, again ignoring polarity differences.

Group-level topographies were backfitted to individual EEGs by a winner-takes-all approach: for each GFP peak, the scalp potential map was compared to each group-level topography and was assigned to the best-matching class based on the spatial correlation. After assigning a microstate class to each GFP peak, these labels were extended to all intervening time frames. The segment boundaries were defined at the midpoints between consecutive GFP peaks (closest neighbor approach), resulting in a continuous segmentation of the EEG.

Finally, the following standard microstates parameters were calculated for each microstate: (1) Mean duration - reflecting synchronous activity of intracortical generators for each occurrence of a particular microstate configuration, and measured in milliseconds (ms) (Khanna et al., 2015); (2) Occurrence rate - referring to the mean number of times a microstate occurred during one second period and interpreted as the tendency of intracortical sources to be synchronously activated (measured in Hertz, Hz), (Khanna et al., 2015); (3) Coverage - reflecting the total percentage of the time frames for which a microstate is accounted (Khanna et al., 2015; Murray et al., 2008); (4) GFP – reflecting the spatial standard deviation of the EEG signal across electrodes at each time point (Murray et al., 2008).

2.5. Statistical analysis

The effects of different tES modalities on EEG microstate dynamics were examined using a series of linear mixed-effects models (LMMs). In all models, stimulation CONDITION (real tES vs. sham) and TIME (pre vs. post) were entered as fixed factors, while participant ID was included as a random grouping factor (e.g., *Duration_MS1 ~ condition * time + (1 | ID)*). Separate models were specified for each real tES–sham comparison, for each microstate class (A, B, C, D), and for each outcome variable (duration, occurrence, contribution, GFP). The primary focus was on the interaction terms, as these indicate stimulation-specific changes (i.e., whether pre-to-post differences varied between real and sham stimulation). All post hoc pairwise comparisons used Satterthwaite's method for degrees of freedom estimation. Holm correction was applied to all post hoc pairwise comparisons within each model.

To directly compare active tES modalities (tDCS, tACS, otDCS), outcomes were baseline- (e.g., *tACS_diff = tACS_post – tACS_pre*) and sham-adjusted (*tACS_diff – Sham_diff*) for each participant. These adjusted outcomes were then analyzed using LMMs with stimulation type (tDCS, tACS, otDCS) as a fixed factor and participant ID as a random factor. Post hoc comparisons were conducted with Holm correction to control for multiple comparisons.

All statistical analyses were carried out using JASP (v0.95) (JASP 2025 Team) and the lme4 package in R (v4.5.1) (Bates et al., 2015).

3. Results

3.1. Microstate topographies and temporal parameters

Four canonical microstate classes - A, B, C, and D - were identified, consistently explaining ~80% of variance (range: 79.99% - 81.28%; without differences between tES conditions or pre-to-post, all $p > .136$). Fig. 1 shows the corresponding topographical representations of microstates in pre- and post-stimulation conditions (panel D). The spatial correlations between microstates extracted pre- and post-tES ranged between 0.72 and 0.97 in corresponding tES conditions and 0.65 to 1 for cross-stimulation (panel E). Therefore, the canonical microstate structure was stable across stimulation conditions and assessments. The descriptive characteristics of microstates, such as duration, occurrence, contribution, and GFP, are provided in the Supplementary Material (Table S1).

The full account of the 2 (CONDITION: real, sham) x 2 (TIME: pre, post) LMMs on EEG microstate measures (duration, occurrence, contribution, and GFP) is provided in the Supplementary material for each of the tES types (Table S2). Below, we first report each active-versus-sham comparison separately and then summarize the direct comparisons between active stimulation modalities using baseline- and sham-adjusted outcomes.

3.2. tDCS effects

A significant CONDITION x TIME interaction was observed for MS A occurrence [$F_{(1123)} = 4.05$, $p = .046$, $\eta_p^2 = 0.03$], and contribution [$F_{((1123)} = 6.07$, $p = .015$, $\eta_p^2 = 0.05$] (see Fig. S1 of the Supplementary material). At baseline, contribution was higher in the sham condition [$t(123) = 4.32$, $p < 0.001$], with a similar trend observed for occurrence [$t(123) = 2.23$, $p = .055$]. Post stimulation increases in MS A measures following tDCS relative to sham abolished the baseline differences (p-values > 0.402).

For MS B, significant interactions were found for duration [$F_{(1123)} = 24.53$, $p < 0.001$, $\eta_p^2 = 0.17$], contribution [$F_{(1123)} = 4.18$, $p = .043$, $\eta_p^2 = 0.03$], and GFP [$F_{(1123)} = 14.62$, $p < 0.001$, $\eta_p^2 = 0.11$], Although baseline duration and contribution were higher in the tDCS condition (p-values <0.002), the main post-tDCS effect was a marked reduction in duration [$t(123) = 3.07$, $p = .003$], relative to sham. Furthermore, with equal baselines, GFP was found to be lower post-tDCS relative to sham [$t(123) = 4.05$, $p < 0.001$].

For MS C, an interaction was observed for occurrence [$F_{(1123)} = 5.84$, $p = .017$, $\eta_p^2 = 0.05$], and GFP [$F_{(1123)} = 6.48$, $p = .012$, $\eta_p^2 = 0.05$]. With equal baselines (p-values > 0.371), higher occurrence [$t(123) = 3.34$, $p = 0.002$] and lower GFP [$t(123) = 2.70$, $p = .016$] were recorded following tDCS relative to sham.

Finally, for MS D significant interaction was observed for duration [$F_{(1123)} = 17.11$, $p < 0.001$, $\eta_p^2 = 0.12$], and GFP [$F_{(1123)} = 31.25$, $p < 0.001$, $\eta_p^2 = 0.20$]. With equal baseline (p-values >0.675), post-stimulation tDCS effects were consistently negative, with shorter duration [$t(123) = 2.84$, $p = .011$] and lower GFP [$t(123) = 3.15$, $p = .004$] relative to sham.

3.3. tACS effects

For MS A, significant CONDITION x TIME interactions were observed for duration [$F_{(1123)} = 5.77$, $p = .018$, $\eta_p^2 = 0.04$], contribution [$F_{(1123)} =$

5.86, p = 0.017, $\eta_p^2 = 0.05$], and GFP [$F_{(1123)} = 7.03, p = .010, \eta_p^2 = 0.05$] (see Fig. S2 of the Supplementary material). At baseline, no differences were found between tACS and sham (all *p*-values > 0.108). In contrast, post-stimulation tACS produced a significantly higher contribution [$t(123) = 2.95, p = .008$] and a trend toward longer duration [$t(123) = 2.26, p = .051$] compared with sham.

For MS B, significant interactions were found for duration [$F_{(1123)} = 25.00, p < 0.001, \eta_p^2 = 0.17$], contribution [$F_{(1123)} = 19.94, p < 0.001, \eta_p^2 = 0.14$], and GFP [$F_{(1123)} = 5.01, p = .027, \eta_p^2 = 0.04$]. For contribution [$t(123) = 2.11, p = .037$] and, on a trend-level duration [$t(123) = 1.93, p = .056$], unequal baselines were observed with higher pre-tACS than pre-sham values. In post-stimulation assessment, however, significantly lower values were observed for all three measures compared to sham [duration $t(123) = 5.14, p < 0.001$; contribution $t(123) = 4.21, p < 0.001$; GFP $t(123) = 2.75, p = 0.014$].

For MS C, significant interactions were found for the measures of duration [$F_{(1123)} = 6.52, p = 0.012, \eta_p^2 = 0.05$] and contribution [$F_{(1123)} = 4.48, p = .036, \eta_p^2 = 0.04$]. At the baseline, no differences between tACS and sham were observed (all *p*-values > 0.445), while both measures showed significantly lower post-stimulation values relative to sham [duration $t(123) = 3.85, p < 0.001$; contribution $t(123) = 3.76, p < 0.001$].

For MS D, significant interactions were found for occurrence [$F_{(1123)} = 6.04, p = .015, \eta_p^2 = 0.05$] and contribution [$F_{(1123)} = 4.70, p < .032, \eta_p^2 = 0.04$]. At the baseline, no differences between tACS and sham were observed (all *p*-values > 0.847). Both measures showed higher post-simulation values relative to sham [occurrence $t(123) = 3.28, p = .003$; contribution $t(123) = 3.10, p = .005$].

3.4. otDCS effects

For MS A significant CONDITION x TIME interactions were observed for measures of duration [$F_{(1123)} = 17.11, p < 0.001, \eta_p^2 = 0.12$], occurrence [$F_{(1123)} = 16.79, p < 0.001, \eta_p^2 = 0.12$], and contribution [$F_{(1123)} = 31.25, p < 0.001, \eta_p^2 = 20$] (see Fig. S3 of the Supplementary material). For all three measures, unequal baselines (all *p*-values <0.003) with higher pre-sham than pre-otDCS values were observed. Conversely, after the stimulation, a higher occurrence [$t(123) = 2.58, p = .011$] was observed relative to sham, as well as a trend-level increase in contribution [$t(123) = 1.77, p = .079$].

For MS B, significant interactions were found for duration [$F_{(1123)} = 49.04, p < 0.001, \eta_p^2 = 0.29$], contribution [$F_{(1123)} = 28.53, p < 0.001, \eta_p^2 = 0.19$], and GFP [$F_{(1123)} = 19.87, p < 0.001, \eta_p^2 = 0.14$]. For all three measures, unequal baselines (all *p*-values <0.022) with higher pre-otDCS in comparison to pre-sham values were recorded. However, the inverse pattern was observed in post-assessment. Namely, shorter duration [$t(123) = 3.15, p = .002$] and lower GFP [$t(123) = 3.98, p < 0.001$] were observed following otDCS compared to sham.

For MS C, significant interactions were found for duration [$F_{(1123)} = 15.26, p < 0.001, \eta_p^2 = 0.11$], contribution [$F_{(1123)} = 12.08, p < 0.001, \eta_p^2 = 0.09$], and GFP [$F_{(1123)} = 5.62, p = .019, \eta_p^2 = 0.04$]. At baseline, no differences were observed between otDCS and sham. Relative to sham, following otDCS, shorter duration [duration $t(123) = 5.53, p < 0.001$], as well as lower contribution [$t(123) = 4.80, p < 0.001$], and lower GFP [$t(123) = 4.53, p < 0.001$] were observed.

For MS D, significant interactions were found for occurrence [$F_{(1123)} = 16.54, p < 0.001, \eta_p^2 = 0.12$] and contribution [$F_{(1123)} = 16.52, p < 0.001, \eta_p^2 = 0.12$]. For both measures, no differences were observed between otDCS and sham at baseline (*p*-values > 0.646). At post-assessment, both occurrence [$t(123) = 5.29, p < 0.001$] and contribution [$t(123) = 5.06, p < 0.001$] showed an increase compared to sham.

3.5. Comparison between tDCS, tACS, and otDCS effects

Across all tES modalities, MS A tended to increase its presence, but the magnitude of facilitation differed significantly between stimulation types (Fig. 2). tACS produced greater facilitation than tDCS on GFP ($t(82) = 3.19, p = .006$), whereas otDCS outperformed tACS on both occurrence ($t(82) = 3.76, p < 0.001$) and contribution ($t(82) = 3.38, p = .002$). Compared with tDCS, otDCS showed stronger facilitatory effects on all MS A measures (duration: $t(82) = 2.77, p = .021$; occurrence: $t(82) = 2.46, p = .032$; contribution: ($t(82) = 3.83, p < 0.001$), and GFP: $t(82) = 2.33, p = .045$).

The overall negative impact on MS B also varied by stimulation type. Relative to tDCS, tACS was associated with a lower occurrence ($t(82) = 2.45, p = .033$), while otDCS produced shorter duration ($t(82) = 4.24, p < 0.001$), lower occurrence ($t(82) = 2.88, p = .015$) lower contribution ($t(82) = 4.72, p < 0.001$). Compared with tACS, otDCS again exerted stronger effects, further decreasing duration ($t(82) = 3.66, p < 0.001$), contribution ($t(82) = 2.85, p = .011$), and GFP (t(82)=4.02, p<.001).

For MS C, the effects of both tACS and otDCS differed significantly from tDCS, each resulting in lowered occurrence ($t(82) = 3.11, p = .005$, $t(82) = 3.99, p < 0.001$, respectively) and contribution ($t(82) = 2.30, p = .048$, $t(82) = 3.85, p < 0.001$, respectively).

Pairwise comparisons confirmed the initially divergent effects of tES modalities on MS D. Namely, statistically significant differences between tDCS and tACS, as well as otDCS, were observed. tACS produced significantly greater duration (t(82) = 3.36, p = .002), occurrence (t(111.73) = 2.87, p = .010), contribution (t(82) = 3.23, p = .004), and GFP (t(82) = 3.96, p < 0.001) compared to tDCS. Finally, otDCS showed the largest facilitation overall, significantly exceeding tDCS on all measures (duration: t(82) = 4.18, p < 0.001), occurrence: t(82) = 3.02, p = .010; contribution: t(82) = 4.44, p < 0.001; and GFP: t(82) = 2.51, p = .028), but differences between otDCS and tACS did not reach statistical significance.

4. Discussion

EEG microstates provide a valuable framework for examining the net effects of brain stimulation, as they capture transient, quasi-stable topographies that reflect the coordinated activity of large-scale functional networks (Tarailis et al., 2024). This network-level perspective is particularly relevant in the context of tES, where low-intensity currents are hypothesized to induce widespread changes in cortical dynamics rather than isolated local effects, given the reduced focality of the applied electric fields (Huang et al., 2017; Opitz et al., 2015; Datta et al., 2009). Although microstate analysis has been increasingly applied in psychiatric and neurological populations, few studies to date have explored how microstates respond to brain stimulation. The present study contributes to this emerging field by directly comparing the immediate aftereffects of the three distinct modalities of tES (tDCS, tACS, and otDCS) on the resting-state EEG microstates in healthy adults. We show that canonical microstates are sensitive to tES-induced neurophysiological changes, and that they are differentially modulated depending on stimulation modality, with otDCS consistently producing the largest effects and showing partial overlap with the effects of both tDCS and tACS. These findings highlight the sensitivity of EEG microstates to detect large-scale network reorganizations induced by brain stimulation and position otDCS as a particularly potent protocol for modulating global brain dynamics.

Across stimulation modalities (tDCS/tACS/otDCS), several consistent patterns emerged. MS A was facilitated by all active protocols, with otDCS producing the strongest increases across duration, occurrence, contribution, and GFP. MS B was consistently suppressed, again most strongly by otDCS, which reduced all parameters beyond the effects of tDCS or tACS. MS C was selectively reduced by theta-oscillatory stimulation (tACS and otDCS). Finally, MS D showed divergent effects: it was suppressed by tDCS but enhanced under theta-oscillatory protocols, with otDCS producing the strongest facilitation. Together, these findings indicate both shared and setting-specific influences of tES on microstate dynamics, with otDCS emerging as the most effective in modulating network-level brain activity.

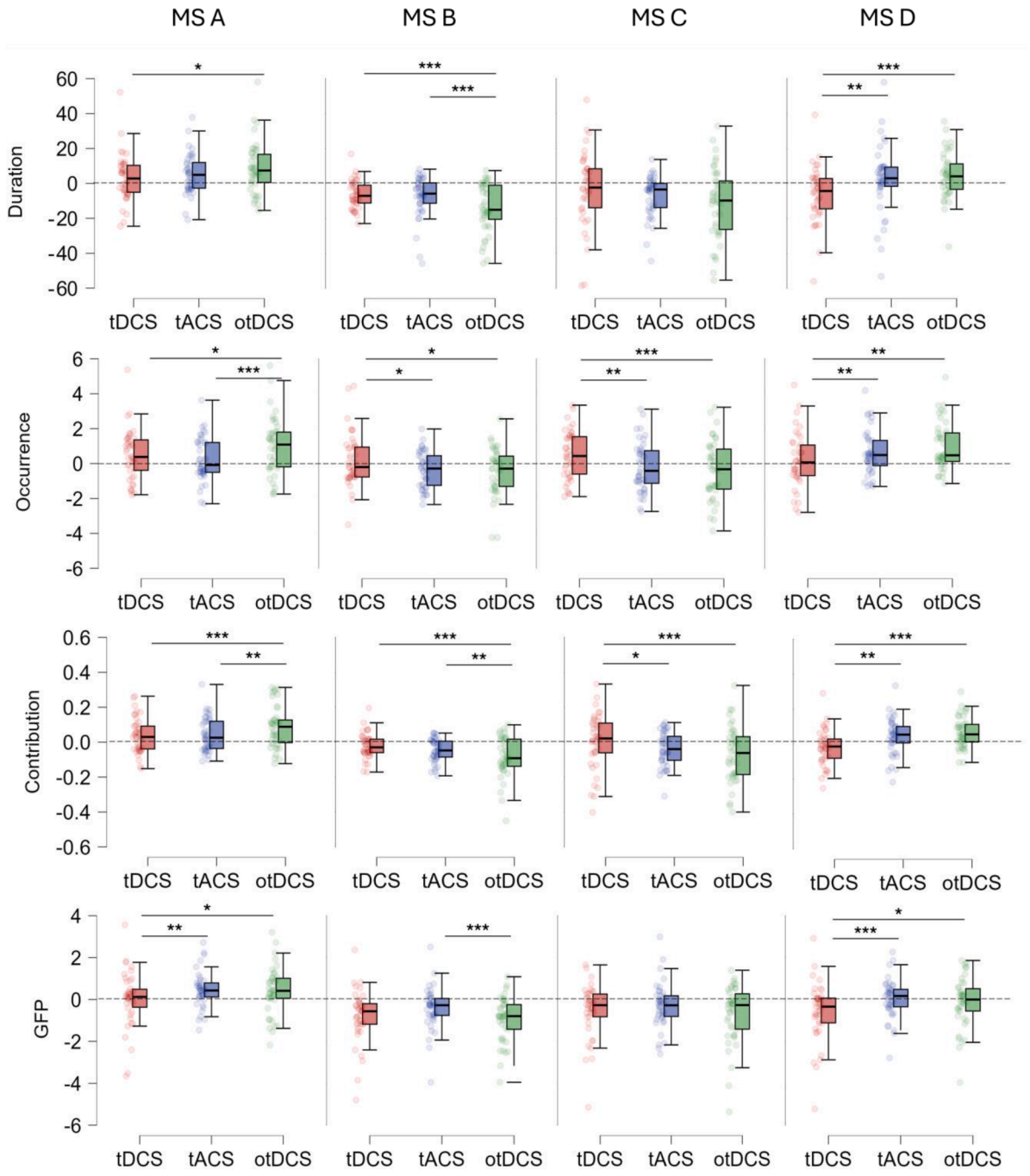

Fig. 2. Differential effects of tDCS, tACS, and otDCS on EEG microstate parameters. *$p < 0.05$, **$p < 0.01$, ***$p < 0.001$. The dotted line represents a reference point for deviations from baseline-corrected sham.

Interpreting our results in functional terms provides further insight into how different stimulation settings shape brain dynamics. MS A, associated with auditory–visual processing and arousal (Britz et al., 2010; Tarailis et al., 2024), was facilitated across all protocols, suggesting that tES broadly enhances sensory readiness and alertness, which may translate into heightened vigilance to external input. This falls in line and explains findings of behavioral studies showing that parietal tDCS and tACS affect attention and vigilance (e.g., Lo et al., 2019; Roy et al., 2015; Kemmerer et al., 2022). MS B, linked to visual self-processing and autobiographical memory (Custo et al., 2017; Tarailis et al., 2024), was consistently suppressed, particularly under oscillatory protocols, indicating a shift away from internally oriented visual–autobiographical states toward externally focused processing. MS C, tied to self-referential and personally significant internal mentation (Tarailis et al., 2024; Milz et al., 2016), was selectively reduced by tACS and otDCS, reflecting a dampening of internally focused cognition and a reallocation of resources toward task-ready states. By contrast, MS D, associated with different cognitive processes - notably executive control and attention-shifting (Tarailis et al., 2024; Seitzman et al., 2017), was enhanced by tACS and otDCS but suppressed by tDCS, suggesting that theta-oscillatory protocols preferentially promote control-related engagement, whereas constant currents exert more stabilizing or inhibitory influences. According to Greenwood et al. (2018), tDCS applied to the dorsal attention network (DAN) should facilitate externally directed cognition by enhancing DAN activity. In our study, however, tDCS reduced the presence of executive-control microstate D,

suggesting a dampening rather than facilitation of externally oriented processing. By contrast, oscillatory protocols (tACS, otDCS) more closely aligned with Greenwood's framework, suppressing DMN-related microstates (B, C) while enhancing MS D, thereby promoting a shift from internally focused to task-ready, externally oriented states.

Our findings also align with the proposed differential effects of tES on cognition (Živanović et al., 2022), which suggest that distinct stimulation protocols may shape cognitive outcomes through distinct neurophysiological mechanisms. The consistent enhancement of MS D under oscillatory protocols (tACS, otDCS) points to a more direct modulatory route, whereby entrainment selectively strengthens executive-control networks. By contrast, tDCS effects appear to operate more indirectly, primarily via suppression of DMN-related microstates (B, C) and facilitation of MS A, reflecting enhanced sensory readiness and attention. The variability of tDCS effects often reported in the behavioral literature (Vergallito et al., 2022) may partly stem from processes leading to the suppression of MS D observed in our data, which could offset potential cognitive benefits by reducing executive-control engagement. In this light, oscillatory protocols may hold greater promise for producing reliable improvements in cognitive outcomes, as they more consistently foster task-ready, control-related network states.

Our results both converge with and extend prior tES–microstate findings. Earlier work has shown that tDCS can increase MS A (sensory/phonological) and MS D (cognitive control) while reducing MS C (self-referential), depending on stimulation site and population (Zhang et al., 2025; Kang et al., 2023). In our study, we similarly observed facilitation of MS A but, in contrast, found suppression of MS D, an executive-control related state, suggesting that while tDCS reliably enhances early sensory-related states, its influence on higher-order control states is more variable. Oscillatory stimulation results were more consistent: γ-tACS has previously been shown to reduce MS C and enhance MS D, reflecting a shift from self-referential toward executive control networks (Gao et al., 2025, 2022). We extend this by demonstrating that tACS and otDCS suppression is not limited to MS C but also includes MS B, particularly under otDCS, indicating a stronger down-regulation of visual-dominant states.

This resonates with findings from single session rTMS studies, which similarly show that stimulation protocols, depending on stimulation site, exert distinct influences on microstates. Qiu et al. (2020) reported that 1 Hz rTMS over the motor cortex increased the duration of all microstates, consistent with a broad stabilization of brain states. In contrast, Croce et al. (2018) found that 1 Hz rTMS over the parietal cortex selectively reduced the occurrence of MS C, indicating targeted modulation of self-referential states, though earlier work also interpreted this effect as salience-related. Interestingly, this parietal effect parallels the reduction of MS C observed with γ-tACS over frontal–parietal regions (Gao et al., 2025, 2022) and with the effects of our theta-oscillatory protocols, suggesting that parietal stimulation, whether magnetic or electrical, consistently targets self-referential networks. In contrast, the tDCS pattern of effects in our study more closely resembles the general stabilization observed with motor cortex rTMS (Guo et al., 2025), underscoring the distinction between constant and oscillatory forms of stimulation.

The differential effects of constant and oscillatory stimulation on microstate dynamics can be interpreted considering their distinct neurophysiological mechanisms. tDCS produces a tonic shift in neuronal membrane potential, biasing populations of neurons toward depolarization or hyperpolarization without imposing rhythmic structure (Nitsche and Paulus, 2000; Stagg and Nitsche, 2011; Reato et al., 2013). Such steady-state modulation is thought to stabilize baseline network configurations, which may explain the broad but relatively modest adjustments observed in our data. In contrast, tACS applies rhythmic alternating currents that interact with ongoing oscillatory activity, promoting phase alignment and frequency-specific entrainment of neural populations (Reato et al., 2013; Antal and Herrmann, 2016). This mechanism enables more selective reorganization of large-scale networks, consistent with the state-specific modulation of MS C and MS D we observed. otDCS, which combines a direct-current offset with an oscillatory component, may therefore combine tonic and oscillatory influences (for in depth discussion see Wischnewski et al., 2026), potentially accounting for its broader and more robust effects on microstates. However, the present study was designed to compare systems-level aftereffects of different waveforms and does not permit direct conclusions about otDCS mechanism of action. A recent report by Guo et al. (2025) further supports the view that otDCS combines the stabilizing effects of tDCS with the entrainment properties of tACS. Authors directly compared 40 Hz otDCS, tACS, and tDCS over the motor cortex and showed that otDCS produced the strongest and most sustained increases in corticospinal excitability, as well as the most pronounced enhancement of large-scale network connectivity measured with TMS–EEG. These effects were interpreted as being consistent with a synergistic mechanism, whereby otDCS simultaneously induces tonic membrane polarization and oscillatory entrainment, thereby amplifying NMDA receptor–dependent plasticity. Our findings are also consistent with this interpretation: otDCS consistently exerted the strongest influence on EEG microstates, modulating all canonical states and producing both tDCS-like stabilization of sensory-related activity and tACS-like reorganization of self-referential and executive-control networks. Supporting evidence from animal models also shows that otDCS, when paired with tDCS, more powerfully enhances endogenous oscillatory activity compared to tDCS alone, especially when matched to intrinsic frequency bands (Al-Tawarah et al., 2023). This indirectly supports our finding that otDCS exerts the most robust modulation of EEG microstates. These distinctions suggest that microstate analysis is sensitive not only to stimulation site and frequency but also to the underlying physics of how different current waveforms shape cortical network dynamics.

Recent evidence from high-definition transcranial direct current stimulation (HD-tDCS) further supports our interpretation. Zhou et al. (2025) found that anodal HD-tDCS over the right dorsolateral prefrontal cortex (dlPFC) reduced MS B and enhanced MS D, mirroring our findings under oscillatory protocols. This indicates that the site and focality of stimulation can influence the effects of constant current protocols. While traditional tDCS induces broad shifts, HD-tDCS may selectively target prefrontal networks, modulating oscillatory dynamics and enhancing executive functions. Overall, waveform, frequency, and focality work together to shape network reorganization, with microstates serving as a sensitive measure of these effects.

Notably, we delivered both tACS and otDCS at a theta frequency that was individual to each participant. This frequency-personalization approach is grounded in the idea that stimulation effects would be maximized when the external current matches intrinsic oscillatory dynamics, thereby increasing the likelihood of phase alignment and effective entrainment (Herrmann et al., 2013; Zaehle et al., 2010; Bjekić et al., 2022; Schmidt et al., 2014). Importantly, we targeted the theta range because of its central role in large-scale brain communication, particularly in coordinating memory and executive-control processes through long-range frontoparietal and hippocampal–cortical networks (Klimesch, 1999; Sauseng et al., 2010). Unlike alpha, which primarily supports sensory inhibition, or gamma, which is more closely linked to local synchronization, theta oscillations provide a temporal scaffold for long-range integration across distributed networks (Kirk and Mackay, 2003; Sattler and Wehr, 2025; Mizuseki et al., 2009). Thus, delivering stimulation at the ITF ensured both frequency specificity and individualized targeting, which may explain why ITF-oscillatory protocols showed selective and consistent modulation of self-referential (MS C) and executive-control (MS D) microstates, in contrast to the more diffuse effects of tDCS. Namely, aligning stimulation with oscillations endogenous to the targeted network likely amplifies resonance effects and facilitates more efficient large-scale reorganization, consistent with evidence that network entrainment is stronger when stimulation frequency is individually tuned (Kemmerer et al., 2022). At the same time, because our design did not include other- or fixed-frequency oscillatory

control conditions, the present findings should not be interpreted as demonstrating theta-band specificity or superiority over other stimulation frequencies.

The observed stimulation-induced modulations also have broader functional and clinical significance. Facilitation of MS A, reflecting sensory readiness and arousal, may help explain why tDCS protocols often produce modest but reliable effects on pain perception and basic sensory processing (Zhang et al., 2025). Suppression of MS B and MS C by oscillatory stimulation suggests a reduction of self-focused and autobiographical mentalization, processes often exaggerated in conditions such as depression and rumination (Tarailis et al., 2024; Milz et al., 2016). Conversely, the enhancement of MS D under tACS and otDCS indicates a strengthening of executive and attentional control networks, consistent with findings that γ-tACS improves working memory performance (Gao et al., 2025). Taken together, these results highlight that oscillatory stimulation may be particularly suited for clinical contexts where self-referential dominance and executive deficits coexist, such as in depression, schizophrenia, or OCD, whereas constant currents may be more effective in modulating sensory readiness or stabilizing overall network dynamics. This possibility, however, remains to be tested directly in clinical populations.

Overall, this study makes several broader contributions. Mechanistically, it provides the first direct evidence that constant and oscillatory tES protocols differentially affect large-scale brain networks, with otDCS bridging polarity-driven and oscillatory mechanisms. To our knowledge, this is also the first study to examine the effects of otDCS on EEG microstates, which necessarily limits the extent of direct comparison to other works. Methodologically, it establishes EEG microstate analysis as a sensitive, temporally precise tool for detecting network-level reorganization induced by neuromodulation. Unlike EEG analyses focused on oscillatory power or connectivity, which capture frequency-specific or pairwise interactions, microstates reflect the rapid succession of whole-brain configurations and thus provide a complementary window into the global coordination of neural activity, making it particularly suited for capturing the broad and distributed effects expected from brain stimulation. Translationally, the results offer proof of concept that microstates from resting-state EEG can serve as practical biomarkers for tracking and differentiating the large-scale effects of distinct tES modalities.

5. Limitations and future directions

Several limitations should be acknowledged. First, our analysis was restricted to the four canonical microstates (A–D). This means that potential distinctions between MS C (self-referential mentation) and MS E (salience-related activity) could not be examined (Tarailis et al., 2024), and some of the effects attributed to MS C may partly reflect overlapping salience-related dynamics. To our knowledge, no existing brain stimulation studies have reported effects on MS E, as most have similarly adopted the four-class solution. Second, the study was conducted in healthy young adults, which limits generalizability to clinical or aging populations where stimulation effects may differ. To that end, it remains an open question whether the oscillatory stimulation would "normalize" altered microstate dynamics in clinical populations or whether those populations would require differently optimized tES protocols. Third, only offline resting-state effects were assessed; the extent to which these modulations translate into task-related brain dynamics or behavioral outcomes remains an open question. Our results suggest that stimulation at individual theta frequencies may enhance the consistency and potency of oscillatory tES effects on large-scale brain networks, but this interpretation should be considered with caution, given that we did not directly compare individualized with fixed-frequency protocols. Similarly, because only one stimulation montage (P3-cheek) and one oscillatory frequency range (theta) were used, it remains an open question whether comparable or very different effects would emerge with other montages, including prefrontal targets, or with non-theta stimulation frequencies. Finally, otDCS is a relatively new protocol, and its mechanisms of action require further validation. Future work should therefore examine microstates using higher-class solutions, extend investigations to clinical groups, and combine EEG with multimodal imaging and behavioral assessments to capture the functional and therapeutic relevance of stimulation-induced network changes more fully.

6. Conclusion

This study demonstrates that EEG microstates provide a sensitive framework for disentangling the network-level effects of different tES modalities. While tDCS primarily modulated sensory-related states in a manner consistent with network stabilization, oscillatory protocols (particularly otDCS) more strongly reorganized self-referential and cognitive control-related states. By conducting the first within-subject, multimodal comparison of tDCS, tACS, and otDCS, we identified both shared and modality-specific influences on canonical microstates, with otDCS exerting the most robust and widespread effects. These findings contribute to understanding of how distinct current waveforms shape large-scale brain dynamics and establish EEG microstates as a promising biomarker for differentiating, optimizing, and monitoring the system level effects of neuromodulation strategies.

Funding

The data for this study have been collected under the MEMORYST grant awared by Science Fund of Republic of Serbia. MŽ and JB receive institutional support from the Ministry of Science, Technological Development and Innovation of the Republic of Serbia (451-03-137/2025-03/200163; 451-03-136/2025-03/200015). IGB, MŽ, SF and JB are engaged in EU-funded HORIZON Collaboration and Support Action TWINNIBS (101059369).

Ethics statement

The study protocol was reviewed and approved by the Ethics Committee of the Institute for Medical Research, University of Belgrade. All participants received written and verbal information about the study procedures and provided written informed consent before participating. Participation was voluntary, and participants could withdraw from the study at any time without consequences. All procedures were conducted in accordance with the Declaration of Helsinki and relevant institutional and ethical guidelines.

Data and code availability statement

The participant-level EEG and behavioral data are not publicly available due to ethical and privacy restrictions. De-identified data may be made available by the corresponding author upon reasonable request, subject to approval by the relevant ethics committee and completion of an institutional data-sharing agreement.

CRediT authorship contribution statement

Inga Grišková-Bulanova: Writing – review & editing, Writing – original draft, Visualization, Methodology, Formal analysis, Conceptualization. **Povilas Tarailis:** Visualization, Formal analysis, Data curation. **Marko Živanović:** Writing – review & editing, Writing – original draft, Visualization, Methodology, Investigation, Formal analysis, Data curation. **Saša Filipović:** Writing – review & editing, Methodology. **Jovana Bjekić:** Writing – review & editing, Writing – original draft, Visualization, Methodology, Investigation, Funding acquisition, Conceptualization.

Declaration of competing interest

The authors declare that they have no known competing financial interests or personal relationships that could have appeared to influence the work reported in this paper.

Supplementary materials

Supplementary material associated with this article can be found, in the online version, at doi:10.1016/j.neuroimage.2026.122007.

References

Agboada, D., Zhao, Z., Wischnewski, M., 2025. Neuroplastic effects of transcranial alternating current stimulation (tACS): from mechanisms to clinical trials. Front. Hum. Neurosci. 19, 1548478.

Al-Tawarah, N.M., Kaptan, Z., Abu-Harirah, H.A., Nofal, M., Almajali, B., Jarrar, S., et al., 2023. Effectiveness of anodal otDCS following with anodal tDCS rather than tDCS alone for increasing of relative power of intrinsic matched EEG bands in rat brains. Brain Sci. 13 (1), 72.

Antal, A., Herrmann, C.S., 2016. Transcranial alternating current and random noise stimulation: possible mechanisms. Neural Plast. 2016, 3616807.

Antal, A., Paulus, W., 2013. Transcranial alternating current stimulation (tACS). Front. Hum. Neurosci. 7, 317.

Bates, D., Mächler, M., Bolker, B., Walker, S., 2015. Fitting linear mixed-effects models using lme4. J. Stat. Softw. 67 (1), 1–48.

Bjekić, J., Paunovic, D., Živanović, M., Stanković, M., Griskova-Bulanova, I., Filipović, S. R., 2022a. Determining the individual theta frequency for associative memory targeted personalized transcranial brain stimulation. J. Pers. Med. 12 (9).

Bjekić, J., Živanović, M., Paunović, D., Vulić, K., Konstantinović, U., Filipović, S.R., 2022b. Personalized frequency modulated transcranial electrical stimulation for associative memory enhancement. Brain Sci. 12 (4).

Britz, J., Van De Ville, D., Michel, C.M., 2010. BOLD correlates of EEG topography reveal rapid resting-state network dynamics. Neuroimage 52 (4), 1162–1170.

Cheng, J., Wang, Y., Tang, Y., Lin, L., Gao, J., Wang, Z., 2024. EEG microstates are associated with the improvement of obsessive-compulsive symptoms after transcranial direct current stimulation. J. Psychiatr. Res. 176, 360–367.

Croce, P., Zappasodi, F., Capotosto, P., 2018. Offline stimulation of human parietal cortex differently affects resting EEG microstates. Sci. Rep. 8 (1), 1287.

Custo, A., Van De Ville, D., Wells, W.M., Tomescu, M.I., Brunet, D., Michel, C.M., 2017. Electroencephalographic resting-state networks: source localization of microstates. Brain Connect. 7 (10), 671–682.

Datta, A., Bansal, V., Diaz, J., Patel, J., Reato, D., Bikson, M., 2009. Gyri-precise head model of transcranial direct current stimulation: improved spatial focality using a ring electrode versus conventional rectangular pad. Brain Stimul. 2 (4), 201–207.e1.

Delorme, A., Makeig, S., 2004. EEGLAB: an open source toolbox for analysis of single-trial EEG dynamics including independent component analysis. J. Neurosci. Methods 134 (1), 9–21.

Elyamany, O., Leicht, G., Herrmann, C.S., Mulert, C., 2021. Transcranial alternating current stimulation (tACS): from basic mechanisms towards first applications in psychiatry. Eur. Arch. Psychiatry Clin. Neurosci. 271 (1), 135–156.

Faul, F., Erdfelder, E., Lang, A.-G., Buchner, A., 2007. G*Power 3: A flexible statistical power analysis program for the social, behavioral, and biomedical sciences. Behav. Res. Methods 39 (2), 175–191.

Filmer, H.L., Dux, P.E., Mattingley, J.B., 2014. Applications of transcranial direct current stimulation for understanding brain function. Trends Neurosci. 37 (12), 742–753.

Gao, B., Suo, D., Yan, T., Zhang, J., Zhang, J., Funahashi, S., et al., 2022. EEG microstate analysis of transcranial alternating current stimulation in healthy people. In: Proceedings of the 2022 16th ICME International Conference on Complex Medical Engineering (CME), pp. 165–168.

Gao, B., Zhang, J., Zhang, J., Pei, G., Liu, T., Wang, L., et al., 2025. Gamma transcranial alternating current stimulation enhances working memory ability in healthy people: an EEG microstate study. Brain Sci. 15 (4), 381.

Gold, M.C., Yuan, S., Tirrell, E., Kronenberg, E.F., Kang, J.W.D., Hindley, L., et al., 2022. Large-scale EEG neural network changes in response to therapeutic TMS. Brain Stimul. 15 (2), 316–325.

Greenwood, P.M., Blumberg, E.J., Scheldrup, M.R., 2018. Hypothesis for cognitive effects of transcranial direct current stimulation: externally- and internally-directed cognition. Neurosci. Biobehav. Rev. 86, 226–238.

Guo, Z., Qiu, H., Li, Y., Wang, S., Gao, Y., Yuan, M., et al., 2025. Gamma oscillatory transcranial direct current stimulation of motor cortex enhances corticospinal excitability and brain connectivity in healthy individuals. Cereb. Cortex. 35 (4), bhaf093.

Hanoglu, L., Toplutas, E., Saricaoglu, M., Velioglu, H.A., Yildiz, S., Yulug, B., 2022. Therapeutic role of repetitive transcranial magnetic stimulation in Alzheimer's and Parkinson's disease: electroencephalography microstate correlates. Front. Neurosci. 16.

Herrmann, C.S., Rach, S., Neuling, T., Strüber, D., 2013. Transcranial alternating current stimulation: a review of the underlying mechanisms and modulation of cognitive processes. Front. Hum. Neurosci. 7.

Huang, Y., Liu, A.A., Lafon, B., Friedman, D., Dayan, M., Wang, X., et al., 2017. Measurements and models of electric fields in the in vivo human brain during transcranial electric stimulation. Elife 6, e18834.

JASP Team. JASP (Version 0.95) [Computer Software]. 2025. Available from: https://jasp-stats.org/.

Kang, J., Fan, X., Zhong, Y., Casanova, M.F., Sokhadze, E.M., Li, X., et al., 2023. Transcranial direct current stimulation modulates EEG microstates in low-functioning autism: a pilot study. Bioengineering 10 (1) (Basel).

Kemmerer, S.K., de Graaf, T.A., ten Oever, S., Erkens, M., De Weerd, P., Sack, A.T., 2022a. Parietal but not temporoparietal alpha-tACS modulates endogenous visuospatial attention. Cortex 154, 149–166.

Kemmerer, S.K., Sack, A.T., de Graaf, T.A., Ten Oever, S., De Weerd, P., Schuhmann, T., 2022b. Frequency-specific transcranial neuromodulation of alpha power alters visuospatial attention performance. Brain Res. 1782, 147834.

Khanna, A., Pascual-Leone, A., Michel, C.M., Farzan, F., 2015. Microstates in resting-state EEG: current status and future directions. Neurosci. Biobehav. Rev. 49, 105–113.

Kirk, I.J., Mackay, J.C., 2003. The role of theta-range oscillations in synchronising and integrating activity in distributed mnemonic networks. Cortex 39 (4), 993–1008.

Klimesch, W., 1999. EEG alpha and theta oscillations reflect cognitive and memory performance: a review and analysis. Brain Res. Rev. 29 (2), 169–195.

Koenig, T., Brandeis, D., 2016. Inappropriate assumptions about EEG state changes and their impact on the quantification of EEG state dynamics. Neuroimage 125, 1104–1106.

Koenig, T., Lehmann, D., Merlo, M.C., Kochi, K., Hell, D., Koukkou, M., 1999. A deviant EEG brain microstate in acute, neuroleptic-naive schizophrenics at rest. Eur. Arch. Psychiatry Clin. Neurosci. 249 (4), 205–211.

Lo, O.Y., van Donkelaar, P., Chou, L.S., 2019. Effects of transcranial direct current stimulation over right posterior parietal cortex on attention function in healthy young adults. Eur. J. Neurosci. 49 (12), 1623–1631.

Michel, C.M., Koenig, T., 2018. EEG microstates as a tool for studying the temporal dynamics of whole-brain neuronal networks: a review. Neuroimage 180 (Pt B), 577–593.

Milz, P., Faber, P.L., Lehmann, D., Koenig, T., Kochi, K., Pascual-Marqui, R.D., 2016. The functional significance of EEG microstates: associations with modalities of thinking. Neuroimage 125, 643–656.

Mizuseki, K., Sirota, A., Pastalkova, E., Buzsáki, G., 2009. Theta oscillations provide temporal windows for local circuit computation in the entorhinal-hippocampal loop. Neuron 64 (2), 267–280.

Murray, M.M., Brunet, D., Michel, C.M., 2008. Topographic ERP analyses: a step-by-step tutorial review. Brain Topogr. 20 (4), 249–264.

Nagabhushan Kalburgi, S., Kleinert, T., Aryan, D., Nash, K., Schiller, B., Koenig, T., 2024. MICROSTATELAB: the EEGLAB toolbox for resting-state microstate analysis. Brain Topogr. 37 (4), 621–645.

Nishida, K., Minami, S., Yamane, T., Ueda, S., Tsukuda, B., Ikeda, S., et al., 2025. A single session of tDCS stimulation can modulate an EEG microstate associated with anxiety in patients with depression. Brain Behav. 15 (5), e70580.

Nitsche, M.A., Paulus, W., 2000. Excitability changes induced in the human motor cortex by weak transcranial direct current stimulation. J. Physiol. 527 (Pt 3), 633–639.

Opitz, A., Paulus, W., Will, S., Antunes, A., Thielscher, A., 2015. Determinants of the electric field during transcranial direct current stimulation. Neuroimage 109, 140–150.

Pascual-Marqui, R.D., Michel, C.M., Lehmann, D., 1995. Segmentation of brain electrical activity into microstates: model estimation and validation. IEEE Trans. Biomed. Eng. 42 (7), 658–665.

Qin, X., Wang, Q., Li, H., Wang, J., Mao, Z., Dong, F., et al., 2025. Effects of tDCS with concurrent cognitive performance targeting the dorsolateral prefrontal cortex and the posterior parietal cortex on EEG microstates in schizophrenia. Schizophr. Res. 277, 117–123.

Qiu, S., Wang, S., Yi, W., Zhang, C., He, H., 2020. Changes of resting-state EEG microstates induced by low-frequency repetitive transcranial magnetic stimulation. Annu. Int. Conf. IEEE Eng. Med. Biol. Soc. 2020, 3549–3552.

Reato, D., Rahman, A., Bikson, M., Parra, L.C., 2013. Effects of weak transcranial alternating current stimulation on brain activity: a review of known mechanisms from animal studies. Front. Hum. Neurosci. 7, 687.

Rousseeuw, P.J., 1987. Silhouettes: a graphical aid to the interpretation and validation of cluster analysis. J. Comput. Appl. Math. 20, 53–65.

Roy, L.B., Sparing, R., Fink, G.R., Hesse, M.D., 2015. Modulation of attention functions by anodal tDCS on right PPC. Neuropsychologia 74, 96–107.

Sattler, N.J., Wehr, M., 2025. Cortex-wide spatiotemporal motifs of theta oscillations are coupled to freely moving behavior. Front. Syst. Neurosci. 19.

Sauseng, P., Griesmayr, B., Freunberger, R., Klimesch, W., 2010. Control mechanisms in working memory: a possible function of EEG theta oscillations. Neurosci. Biobehav. Rev. 34 (7), 1015–1022.

Schmidt, S.L., Iyengar, A.K., Foulser, A.A., Boyle, M.R., Fröhlich, F., 2014. Endogenous cortical oscillations constrain neuromodulation by weak electric fields. Brain Stimul. 7 (6), 878–889.

Seitzman, B.A., Abell, M., Bartley, S.C., Erickson, M.A., Bolbecker, A.R., Hetrick, W.P., 2017. Cognitive manipulation of brain electric microstates. Neuroimage 146, 533–543.

Stagg, C.J., Nitsche, M.A., 2011. Physiological basis of transcranial direct current stimulation. Neuroscientist 17 (1), 37–53.

Tarailis, P., Koenig, T., Michel, C.M., 2024. Griškova-Bulanova I. The functional aspects of resting EEG microstates: a systematic review. Brain Topogr. 37 (2), 181–217.

Tarailis, P., Šimkutė, D., Koenig, T., 2021. Griškova-Bulanova I. Relationship between spatiotemporal dynamics of the brain at rest and self-reported spontaneous thoughts: an EEG microstate approach. J. Pers. Med. 11 (11), 1216.
Vass, Á., Farkas, K., Lányi, O., Kói, T., Csukly, G., Réthelyi, J.M., et al., 2025. Current status of electroencephalography microstate in psychiatric disorders: a systematic review and meta-analysis. Biol. Psychiatry Cogn. Neurosci. NeuroimAging.
Vergallito, A., Feroldi, S., Pisoni, A., Romero Lauro, L.J., 2022. Inter-individual variability in tDCS effects: a narrative review on the contribution of stable, variable, and contextual factors. Brain Sci. 12 (5), 522.
Vulić, K., Bjekić, J., Paunović, D., Jovanović, M., Milanović, S., Filipović, S.R., 2021. Theta-modulated oscillatory transcranial direct current stimulation over posterior parietal cortex improves associative memory. Sci. Rep. 11 (1), 3013.
Wischnewski, M., Alekseichuk, I., Opitz, A., 2023. Neurocognitive, physiological, and biophysical effects of transcranial alternating current stimulation. Trends Cogn. Sci. 27 (2), 189–205. https://doi.org/10.1016/j.tics.2022.11.013.
Wischnewski, M., Ogircin, M.A., Filipović, S.R., Antal, A., Bjekić, J., 2026. Neurophysiological and behavioral effects of oscillatory transcranial direct current stimulation (otDCS). J. Neurosci. Methods 430, 110723.
Woods, A.J., Antal, A., Bikson, M., Boggio, P.S., Brunoni, A.R., Celnik, P., et al., 2016. A technical guide to tDCS, and related non-invasive brain stimulation tools. Clin. Neurophysiol. 127 (2), 1031–1048.
Zaehle, T., Rach, S., Herrmann, C.S., 2010. Transcranial alternating current stimulation enhances individual alpha activity in human EEG. PLoS One 5 (11), e13766.
Zanesco, A.P., 2020. EEG electric field topography is stable during moments of high field strength. Brain Topogr. 33 (4), 450–460.
Zhang, J., Li, Y., Liu, X., Zhang, J., Fan, J., Zhong, D., et al., 2025a. Brain microstate features of patients with depression: a transcranial magnetic stimulation and electroencephalographic (TMS-EEG) study. Psychiatry Res. 351, 116616.
Zhang, Y., Li, X., Qiu, S., Jin, R., Peng, W., 2025b. Preemptive transcranial direct current stimulation mitigates susceptibility to persistent pain. Commun. Biol. 8 (1), 865.
Zhou, Y., Liu, P., Chen, F., Chen, L., 2025. The changes of EEG microstate maps in response to high-definition transcranial direct current stimulation. Cogn. Affect. Behav. Neurosci. 25, 1684–1693.
Živanović, M., Bjekić, J., Konstantinović, U., Filipović, S.R., 2022. Effects of online parietal transcranial electric stimulation on associative memory: a direct comparison between tDCS, theta tACS, and theta-oscillatory tDCS. Sci. Rep. 12 (1), 14091.